Relationship between the ability to control liquid crystal alignment and wetting properties of calix[4]resorcinarene monolayers

Sang-Keun Oh, Masaru Nakagawa and Kunihiro Ichimura*

Chemical Resources Laboratory, Tokyo Institute of Technology, 4259 Nagatsuta, Midori-ku, Yokohama, 226-8503, Japan. E-mail: kichimur@res.titech.ac.jp; Tel: +81-45-924-5266; Fax: +81-45-924-5276

This paper describes the correlation between the ability to control nematic liquid crystal (LC) alignment and wetting properties of mixed monolayers formed by coadsorption of two *O*-octacarboxymethylated calix[4]resorcinarenes (CRA-CMs) with either perfluorooctyl- or octylazobenzene units. Photoirradiation of CRA-CM monolayers induces reversible photoisomerization reaction of the surface azobenzenes, which causes changes in LC alignment and wettability of the monolayers. The photogenerated LC alignments are considerably influenced by the surface compositions of the mixed monolayers. When LC cells fabricated with substrate plates modified with single-component monolayers of CRA-CM with *p*-octylazobenzenes are subjected to oblique irradiation with non-polarized UV light, the orientation of LC molecules is changed from homeotropic to homogeneous alignments tilting toward the direction of light propagation. In contrast, single-component and mixed monolayers of CRA-CM with *p*-perfluorooctylazobenzenes cause homeotropic alignments and tilted alignments with high pretilt angles, respectively. The level of photoisomerization and surface free energy of the CRA-CM monolayers are not a sufficient condition to cause the contrasting alignment behaviors. We conclude that the molecular-level morphology and/or fluidity of the monolayer surfaces of CRA-CMs, which is deduced from the contact angle hysteresis of anisotropic liquids for the surfaces, is the most significant factor to induce the LC alignment alterations observed.

Introduction

Alignment of liquid crystals (LCs) on a solid substrate is governed by physicochemical interactions at the LC/substrate interface.[1,2] This indicates that changes in physicochemical states of an outermost surface lead to alterations of LC alignment. The chemical modifications of substrate surfaces with long-chain alkyl silylating agents and the unidirectional rubbing treatment of polymer thin films are well-known examples to give homeotropic (perpendicular to the substrate surface) and homogeneous (uniaxially parallel) LC alignment, respectively.[2] Conversely, nematic LC droplets placed on organic surfaces were used to characterize the structure of the surfaces by observing their optical textures.[3–5] Although there have been continuous efforts to elucidate the origin of LC alignment behavior, the detailed mechanisms are still not completely understood.[6–8] The photochemical approaches to control the alignment of LCs on the basis of command surfaces have shed light on the elucidation of a working mechanism of LC alignment in molecular levels, because structural as well as orientational changes of molecules are operative specifically at outermost surfaces, which can be well characterized.[9,10] It has been revealed that photoisomerization of azobenzene units incorporated in command surfaces such as self-assembled monolayers (SAMs) of silane derivatives,[11] spin-coated films of polymers[12] and Langmuir–Blodgett films[13] can regulate the alignment of LCs reversibly. A typical example of the photochemical system involves reversible switching between homeotropic and homogeneous alignments upon alternating irradiation of azobenzenes tethered to substrate surfaces with UV and visible light.[11] The photoirradiation induces geometrical transformations as well as polarity changes of the azobenzene units; the dipole moment of rod-shaped *E*-configurations is lower than that of bent-shaped *Z*-configurations. Recently, we have also reported that three-dimensional control of LC photoalignment is possible by the orientational

alteration of azobenzenes when oblique irradiation is carried out with non-polarized light.[14,15] In this procedure, azobenzenes reorient toward the direction in parallel with the light propagation so that the orientational direction of the chromophores is controlled simply by the incident direction of light for photoisomerization. Accordingly, physicochemical properties of a substrate surface comprising azobenzene units are precisely manipulated by appropriate choices of light properties including wavelength, polarization and incident angles. The photochemically operative surfaces thus should offer unique opportunities to deepen fundamental understanding of interfacial interactions occurring at an LC/substrate interface.

Characteristics of wetting of a solid surface provide a wide range of information on properties of the surface.[16] Contact angles of probe liquids on an organic solid surface are remarkably sensitive to chemical compositions and physical structures of the outermost surfaces of a few angstroms in thickness.[17] Although the interpretation of absolute contact angle values obtained from only one system is not always straightforward, the comparisons of data among similar systems have been proved to be invaluable for elucidating characteristics of organic surfaces.[18,19] It has been suggested that changes in molecular-level structures of SAMs, such as adsorption density and structural heterogeneity, critically influence contact angles of liquids on the surfaces.[18]

In this paper, we compare the LC alignment behavior assisted by a photoresponsive surface with wettability of the surface in order to explore the working mechanism of the photoinduced LC alignment. Whereas previous studies have demonstrated the correlation between LC alignment behavior and wettability by using different surfaces which have fixed chemical compositions,[20,21] the results we report are the comparisons of the same surfaces with different photoisomeric states. We use two *O*-octacarboxymethylated calix[4]resorcinarenes (CRA-CMs; **1** and **2** in Fig. 1) incorporating either
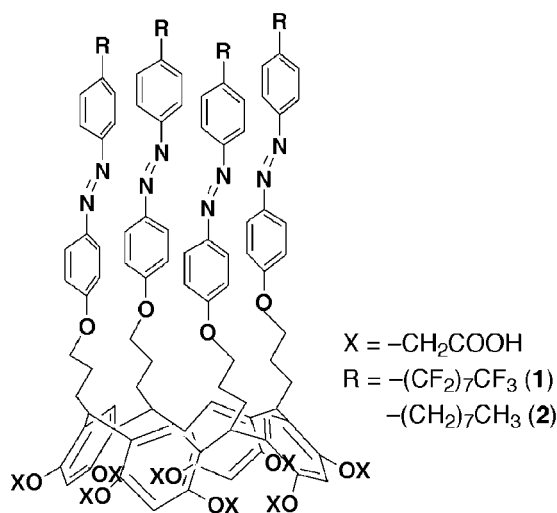
Fig. 1 Chemical structure of CRA-CM derivatives.

perfluorooctyl- or octylazobenzene units as photoresponsive adsorbates. Mixed monolayers composed of two CRA-CMs are formed by exposing an aminated silica substrate to solutions containing mixtures of the CRA-CMs. The coadsorption of **1** and **2** provides a method for generating photoresponsive surfaces exhibiting varied surface compositions and levels of photoisomerization which would influence both the photoinduced LC alignments and wetting properties of the surfaces.

Experimental

Materials

CRA-CMs were synthesized through the Williamson coupling of 2,8,14,20-tetrakis(3-iodopropyl)-4,6,10,12,16,18,22,24-octakis(ethoxycarbonylmethoxy)calix[4]arene with the corresponding 4-phenylazophenol according to our previous report.[22] Nematic LCs of NPC-02 ($T_{NI} = 35.0 \,^{\circ}C$, relative permittivity, $\Delta \varepsilon = -0.1$), a binary mixture of alkoxyphenylcyclohexane derivatives, and 5CB ($T_{NI} = 35.4 \,^{\circ}C$, $\Delta \varepsilon = 11.0$) were kindly donated by Rodic Co., Ltd. A nematic LC of MLC-6608 ($T_{NI} = 90.0 \,^{\circ}C$, $\Delta \varepsilon = -4.2$) was purchased from Merck Japan, Ltd.

Monolayer preparation and fabrication of LC cell

A fused silica substrate was ultrasonically cleaned in a piranha solution (7 : 3 concentrated H_2SO_4–30% H_2O_2) for 1 h, washed with copious amounts of deionized water and subsequently with acetone and dried *in vacuo* (*WARNING: piranha solution should be handled with caution; it has detonated unexpectedly*). After cleaning, the substrate was immersed immediately in a solution of freshly distilled (3-aminopropyl)diethoxymethylsilane (0.25 g) in dry toluene (25 g) for 1 h at 25 °C. The substrate was washed with dry toluene, baked for 30 min at 120 °C, sonicated in toluene and methanol for 2 min each and finally dried *in vacuo*. The aminosilanized substrate was immersed in a 1×10^{-4} mol dm^{-3} THF solution containing CRA-CM (**1** or **2**) for 30 min at 40 °C. A single-component CRA-CM monolayer tethered to the silica substrate was obtained after rinsing thoroughly with THF and dried for 30 min at 80 °C. A mixed monolayer containing **1** and **2** was prepared by the immersion in their mixed solutions with molar ratios of 1 : 1, 1 : 2 and 1 : 4, in which the total concentration of CRA-CMs was 1×10^{-4} mol dm^{-3}. Patterned CRA-CM monolayers were prepared by a microcontact printing method.[23,24] A solution of **2** (5×10^{-5} mol dm^{-3} in ethanol) was filtered through a 0.2 μm filter on to the patterned poly(dimethylsiloxane)

elastomeric stamp. The solution remained in contact with the stamp for 30 s. The excess liquid was removed under a stream of nitrogen. The inked stamp was placed gently on an aminosilanized silica surface. The stamp was left in contact with the substrate for 30 s. For the formation of a surface patterned with two components, the stamped surface was washed with a solution containing **1** to derivatize regions not imprinted by stamping.

A vacant LC cell was fabricated with a pair of the CRA-CM-modified substrates, which were separated by two strips of PET spacers of 25 μm in thickness. A nematic LC in an isotropic phase was injected by capillary action to give a LC cell.

Photoirradiation

Light sources of UV light (365 nm) and visible light (436 nm) were obtained from a 200 W Hg-Xe lamp (San-ei Electric, Supercure-203S) by passing through suitable combinations of glass filters. An LC cell was obliquely irradiated with non-polarized UV light, whose incident angle was set at an angle of 30° from the surface normal, as shown in Fig. 4.

Physical measurements

UV-VIS spectra were recorded on a weak absorption spectrophotometer (JASCO, MAC-1). Conoscopic interference figures were recorded on a polarized optical microscope (Olympus, BH-2) equipped with a high gain color camera (Flovel, HCC-600). XPS spectra were taken on a Shimadzu ESCA3200 spectrometer, which had a Mg Kα line source (1253.6 eV). Survey spectra were performed at a resolution of 1 eV, and quantitative surface compositions of the CRA-CM-modified substrates were determined by the integration of slower scans operated at a resolution of 0.1 eV. The binding energies were calibrated by the C(1 s) peak (284.6 eV). A photogenerated pretilt angle of LCs was determined by the crystal rotation method.[25] A polarization-modulated transmission ellipsometer[26] (JASCO, BFA-150) equipped with a He–Ne laser beam and a photoelastic modulator (PEM) operating at a modulation frequency of 50 kHz was used. Two parameters of phase difference angle and relative amplitude ratio for an LC cell were measured by rotating the LC cell from –60 to 60° to calculate pretilt angles. Advancing and receding contact angles were measured with a contact angle meter (Kyowa Interface Science, SA-11) in air at room temperature (23 °C). Two methods of extension/contraction and sliding angle were employed for probe liquids of water and NPC-02, respectively. Each contact angle reported here represents the average of 5–10 measurements made on different areas of the sample surface, with an error of $\pm 2°$. Contact angles for the *Z*-state correspond to contact angles in a photostationary state after UV light irradiation.

Results and discussion

Monolayer preparation

Monolayers of **1** and **2** were prepared by the chemisorption through electrostatic interactions between aminosilanized substrates and CRA-CMs. Mixed CRA-CM monolayers were formed by coadsorption of **1** and **2** in three kinds of solutions with different molar ratios [$\chi(\mathbf{1})_{\text{solution}} = 0.50$, 0.33, 0.20 for the mixed monolayer of **1** and **2**, where $\chi(\mathbf{1})_{\text{solution}} = [\mathbf{1}]_{\text{sol}} / ([\mathbf{1}]_{\text{sol}} + [\mathbf{2}]_{\text{sol}})$]. Occupied areas of **1** and **2** in single-component monolayers, estimated from UV-VIS measurements under assumption that their absorption coefficients in solution are equal to those in monolayers, were 2.2 and 2.3 nm^2 molecule^{-1}, respectively.[27] We confirmed that the surface density of CRA-CM in the three kinds of mixed monolayers is similar to that of the single-component monolayers. The chemical composition of the mixed
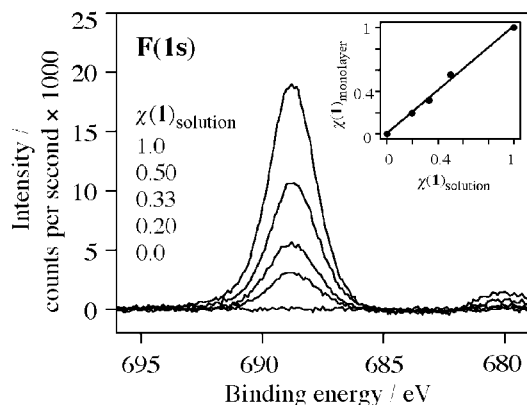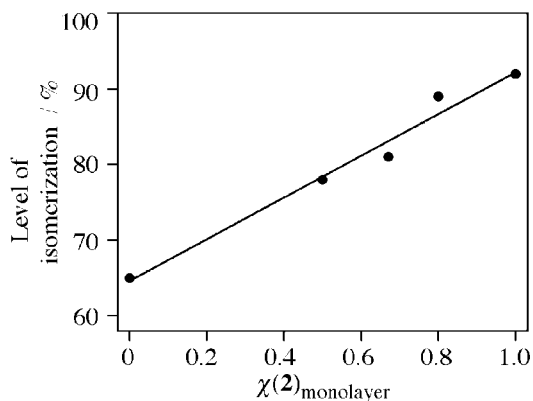
Fig. 2 XPS spectra of the F(1 s) region of mixed CRA-CM monolayers of $\chi(\mathbf{1})_{\text{solution}} = 1.0, 0.50, 0.33, 0.20, 0.$ $\chi(\mathbf{1})$ represents the molar fraction of **1** in solutions or on monolayers. The inset shows the relation of the chemical compositions in solutions and on monolayers.

Fig. 3 Level of E-to-Z photoisomerization of mixed monolayers formed from **1** and **2** as a function of $\chi(\mathbf{2})_{\text{monolayer}}$.

monolayers was determined by XPS (Fig. 2). The area ratios of F(1 s) peaks arising from perfluorooctylated CRA-CM (**1**) in the mixed CRA-CM monolayers were well consistent with the molar ratios of solutions for the chemisorption, $\chi(\mathbf{1})_{\text{solution}}$, even though the solubility of two CRA-CMs in THF was slightly different. This is because adsorption isotherms are determined critically by the high reactivity of carboxylic groups of CRA-CM molecules with amino residues on the silanized surface through acid–base interactions, irrespective of the nature of p-substituents of the azobenzene.

The CRA-CM monolayers have two characteristics worthy of note.[27] First, the monolayer exhibited high desorption-resistance toward polar solvents because of the electrostatic interaction between CRA-CM molecules and the aminosila-nized surface. This fact enabled us to carry out reliable contact angle measurements for water. Second, as noted above, the occupied areas for **1** and **2** in the monolayers are 2.2 and 2.3 nm^2 molecule^{-1}, respectively. These values are not far from the base area of CRA-CM (1.7 nm^2 molecule^{-1}), estimated from π–A isotherm measurements. This observation suggests that there is sufficient free volume in the upper molecular layers consisting of four azobenzene residues ($0.25 \times 4 = 1.00$ nm^2 molecule^{-1}) attached to the lower rim of the cyclic skeleton of CRA-CM.[28] The free volume would result in an increase in the number of *gauche* bonds and a loss of orientational order at the outermost monomolecular layer. Accordingly, it is expected that CRA-CM monolayers show lower contact angle values than those of the densely packed SAMs.[18e]

Photochemistry of monolayers

Our previous studies revealed that the azobenzene embedded in a chemisorbed monolayer of **2** displays 92% of E-to-Z conversion on irradiation with non-polarized UV light.[27] On the other hand, a monolayer of **1** showed 65% of E-to-Z conversion, though occupied areas of both CRA-CMs are not much different from each other.[27] This is most likely due to the steric restriction enhanced by perfluorooctyl substituents, which have a larger cross-sectional area (*ca.* 0.29 nm^2) when compared with octyl ones (*ca.* 0.20 nm^2).[29,30] For mixed monolayers composed of **1** and **2**, the level of E-to-Z photoisomerizability increased in a linear manner with an increase in the fraction of **2**, as shown in Fig. 3. This result indicates that the photoisomerizability is well interpreted simply by an average expression provided by the chemical composition of each component. The coadsorption of CRA-CMs thus offers a simple means of tailoring the possible surface parameters that influence the LC alignments, including dipole moment (long-ranged interaction) and molecular-level geometry (short-ranged interaction) of the outermost molecular

layer.[21a] We discuss the E-to-Z photoisomerizability of azobenzene units in the monolayers in relation to photoinduced LC alignment in the following section.

Photogenerated LC alignments

The photogenerated alignments of LC filled in cells modified with CRA-CM monolayers were confirmed by both conoscopic observation and $\sin \Delta$ values measured by transmission ellipsometry.[25,26] Fig. 4 shows the setup for light irradiation and LC alignment measurements. Conoscopic interference features of LC cells, whose walls are modified with CRA-CM monolayers, filled with NPC-02 are shown in Fig. 5. Before photoirradiation, all LC cells surface-modified with either single-component or mixed CRA-CM monolayers displayed homeotropic alignment, as shown in Fig. 5(a). When the LC cells were subjected to irradiation with oblique non-polarized visible light, no detectable change in LC alignment was observed (data not shown), in contrast to the previous report[14] that oblique irradiation of thin films of polymers with azobenzene side chains with visible light results in the generation of tilting of LC molecules. This observation may be associated with the limited mobility of the azobenzene units of CRA-CMs which are firmly fixed in the silica substrate, in contrast to the azobenzene side chains tethered to an amorphous polymer backbone of spin-cast films. Fig. 5(b) shows changes in conoscopic features of the LC cells after irradiation with non-polarized UV light at an incident angle of 30° from surface normal. The photoirradiation with non-polarized UV light brought about the tilting of
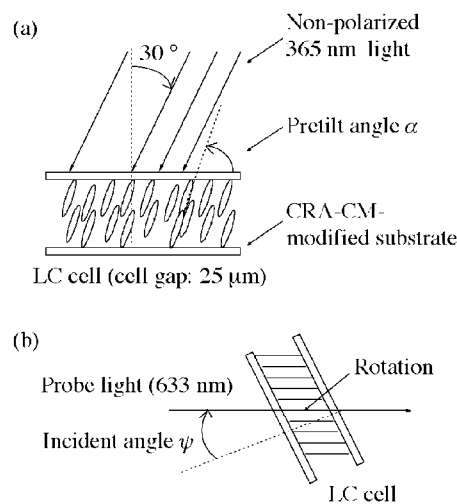

Fig. 4 Illustrative representation of experimental setups for (a) light irradiation and (b) pretilt angle measurements.
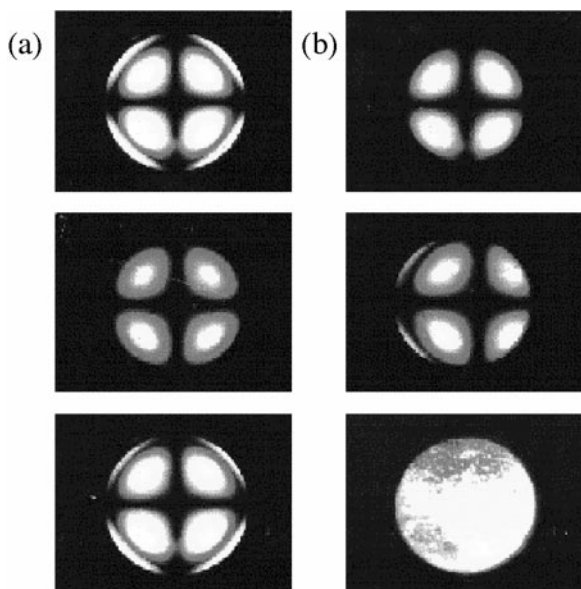
Fig. 5 Conoscopic interference figures of LC cells (NPC-02), the walls of which were modified with mixed monolayers of $\chi(\mathbf{2})_{\mathrm{monolayer}}=0$ (upper), 0.8 (middle) and 1.0 (lower) before (a) and after (b) exposure to UV light of a 1.0 J cm^{-2} exposure dose.

the LC director toward the direction of light propagation without any deterioration of optical quality of homogeneous alignment. The conoscopic features observed indicate that single-component monolayers of **1** and **2** cause homeotropic and homogeneous alignments, respectively, while mixed monolayers of $\chi(\mathbf{2})_{\mathrm{monolayer}}=0.80$, where $\chi(\mathbf{2})_{\mathrm{monolayer}}=$ $[\mathbf{2}]_{\mathrm{monolayer}}/([\mathbf{1}]_{\mathrm{monolayer}}+[\mathbf{2}]_{\mathrm{monolayer}})$, lead to tilted alignments. The contrasting behaviors of LC alignments induced by monolayers of **1** and **2** can be clearly observed by using a LC cell formed from a patterned substrate with areas of the two monolayers. Fig. 6 shows polarized microscopic images of a LC cell fabricated with the patterned substrates before and
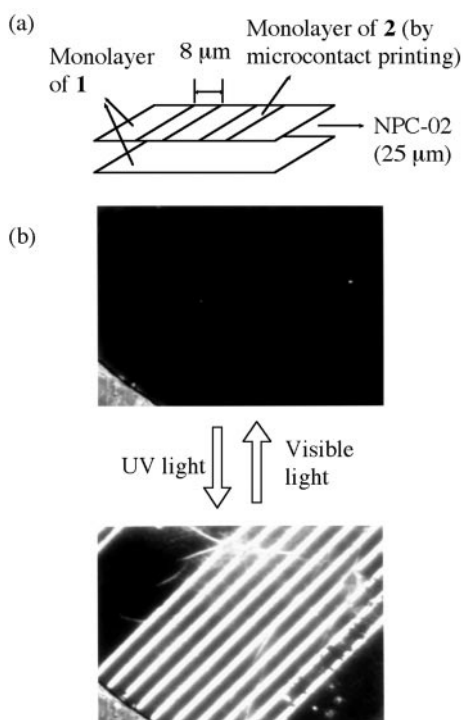

Fig. 6 (a) Schematic illustration of an LC cell fabricated with substrate plates modified with patterned CRA-CM layers generated by microcontact printing. (b) Polarized micrographs of the LC cell before and after oblique irradiation with non-polarized UV light.

after UV light irradiation. The patterned substrates were prepared by a microcontact printing method with a solution of **2**, followed by washing with a solution containing **1** to derivatize regions not imprinted by stamping.[23,24] Before UV irradiation, the LC cell filled with NPC-02 showed a homeotropic alignment uniformly. Upon oblique irradiation with non-polarized UV light, the patterned changes in LC alignment of the LC cell consisting of 8 μm width lines could be imaged by the selective alignment changes of the regions derivatized with **2** from homeotropic to homogeneous alignments.

Precise changes in LC alignments on CRA-CM monolayers upon oblique irradiation with UV light could be followed by a crystal rotation method.[25,26] Fig. 7 summarizes the photogenerated pretilt angle values of LCs as a function of mixing ratios of **1** and **2** after oblique irradiation with non-polarized UV light of a 0.5 J cm^{-2} exposure dose. The pretilt angle values were calculated by fitting a theoretical curve to crystal rotation signals obtained from the transmission ellipsometry measurements. Three kinds of nematic LCs, 5CB, NPC-02 and MLC-6608, whose dielectric anisotropies are positive, zero and negative in sign, respectively, were used to elucidate the dielectric effect of LCs on their alignment transition.[2] A prominent observation for the photogenerated LC alignments is that the LC tilting is considerably influenced by the surface compositions of monolayers denoted as $\chi(\mathbf{2})_{\mathrm{monolayer}}$. First, the homeotropic LC alignments of LC cells of single-component monolayers of **1** ($\chi(\mathbf{2})_{\mathrm{monolayer}}=0$) are essentially not changed after the photoirradiation, irrespective to the nature of LCs filled. Second, in the case of mixed monolayers ($\chi(\mathbf{2})_{\mathrm{monolayer}}=0.50$, 0.67 and 0.80), high pretilt angles are generated in the direction of light propagation. Thirdly, the oblique photoirradiation of single-component monolayers of **2** ($\chi(\mathbf{2})_{\mathrm{monolayer}}=1.0$) results in homogeneous alignments (low pretilt angles) for 5CB and NPC-02, while cells filled with MLC-6608 give rise to non-homogeneous alignment, so that pretilt angle measurements fail.

The quantitative analysis of photogenerated pretilt angles of LCs on CRA-CM monolayers leads us to eliminate two factors that are plausibly responsible for the LC alignments observed. First, if the photoinduced LC alignment is governed critically by the level of *E*-to-*Z* photoisomerization (Fig. 3), pretilt angles should decrease in a linear manner with an increase in $\chi(\mathbf{2})_{\mathrm{monolayer}}$. This is not the case, however, because a sharp transition in LC alignment is observed when $\chi(\mathbf{2})_{\mathrm{monolayer}}$ is 0.80 or larger. Therefore, we conclude that the level of photoisomerization does not exclusively determine the LC photoalignment changes. Second, because the dipole–dipole interactions between a nematic LC and an outermost surface are certainly important in LC alignment,[2] the photoinduced alignment changes can reflect the level and direction of
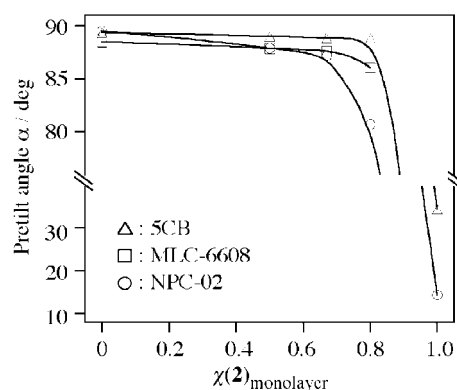

Fig. 7 Photogenerated pretilt angles of LCs in LC cells surface-modified with mixed monolayers of **1** and **2** after oblique irradiation with non-polarized UV light of a 0.5 J cm^{-2} exposure dose as a function of $\chi(\mathbf{2})_{\mathrm{monolayer}}$.

dielectric anisotropy of LCs. Indeed, some examples have been reported to present alignment transitions when LCs with opposite signs of dielectric anisotropy were used; nematic HCB (*p*-heptyl-*p'*-cyanobiphenyl, positive $\Delta\varepsilon$) is aligned perpendicularly to a substrate surface treated with dicarboxylatechronium complexes, while MBBA (*p*-methoxybenzylidene-*p'*-butylaniline, negative $\Delta\varepsilon$) in parallel with it.[31] As shown in Fig. 7, however, the three kinds of LCs, 5CB, NPC-02 and MLC-6608, on the CRA-CM monolayers showed a similar tendency in the photoalignment changes, nevertheless they have positive, nearly zero and negative dielectric anisotropy, respectively. What is clear from the experimental results is that the dipole–dipole interactions between LC molecules and alkylazobenzene residues at the outermost surface are also not responsible for the alignment transition.

Photoinduced changes in contact angle

From the viewpoint that both LC alignment and wettability reflect directly the nature of the outer region of surfaces, we focused our attention on the relationship between the feature of the surface-assisted LC photoalignment and the wettability of CRA-CM monolayers. Fig. 8 shows advancing (θ_a) and receding (θ_r) contact angles for water and NPC-02 on mixed monolayers formed from **1** and **2** before and after oblique irradiation with UV light as a function of $\chi(\mathbf{2})_{monolayer}$. We note that NPC-02 is the same liquid as used for the LC alignment. Although it has been known that it takes a considerable time for an LC droplet to reach an equilibrium with a solid surface,[32] drifting in a contact angle of NPC-02 with time was not detected in our experiments. It is very likely that the degree of drifting with time is within the limits of experimental errors. The results of contact angle measurements are summarized as follows. First, the photoisomerization results in a decrease of θ_a for both water and NPC-02 because polar *Z*-isomers of the azobenzenes are formed at the outermost surface.[33,34] Second, θ_a values for both water and NPC-02 on monolayers decrease with the increment of $\chi(\mathbf{2})_{monolayer}$.[35,36] This is consistent with lower surface densities of perfluoroalkyl groups at higher $\chi(\mathbf{2})_{monolayer}$. Note here that θ_a values for monolayers derived from **1** and **2** are smaller than those observed for densely packed alkanethiolate SAMs; perfluoroalkyl and alkyl SAMs display θ_a(water) = 118° and 112°, respectively,[17a] while the values of θ_a(water) for monolayers of **1** and **2** are 116° and 94°, respectively. Such
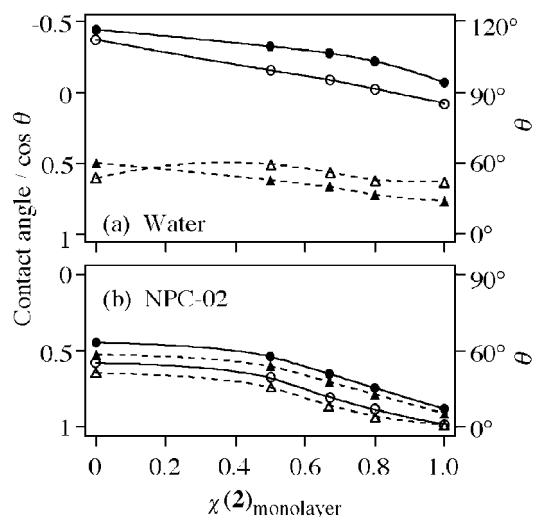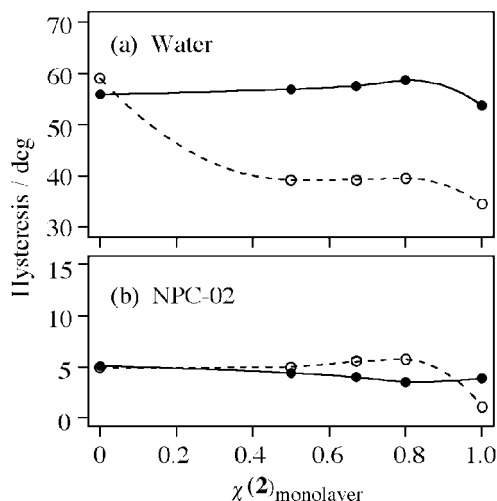
difference arises from the loose packing of both of the *p*-substituents in the chemisorbed CRA-CM monolayers, because the surface density of azobenzene moieties bearing these substituents is determined specifically by the CRA-CM framework, as described above. Thirdly, there is no marked break in all of the contact angle changes as a function of $\chi(\mathbf{2})_{monolayer}$, in particular for monolayers after UV irradiation. This result indicates that the LC photoalignment generation (Fig. 7) cannot be interpreted simply by surface energies that are responsible for the contact angle changes.[20,37]

Photoinduced changes in contact angle hysteresis

A principal observation in wetting properties of CRA-CM monolayers was that the hysteresis in contact angle ($\theta_a - \theta_r$) is largely altered upon photoirradiation. Although uncertainty remains until now, the physical origin of contact angle hysteresis has been considered to be associated with the roughness and the heterogeneity of a solid surface in the absence of mechanical and chemical equilibria.[16] Israelachvili and co-workers suggested that hysteresis arises from the molecular rearrangement occurring at the solid–liquid interfaces after coming into contact.[38,39] Schwartz proposed the concept of *intrinsic contact angle hysteresis* defined as hysteresis that cannot be ascribed to the roughness, heterogeneity or penetrability of a solid surface.[40]
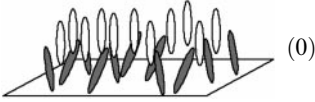
Fig. 9 shows the hysteresis in contact angles for water and NPC-02 as a function of the surface composition. Interestingly, the hysteresis for water was much larger than that for NPC-02. We interpret this large hysteresis for water to reflect the extent of the liquid-induced molecular reorganization. Because water can interact with azobenzenes containing *p*-oxy substituents through hydrogen bonding,[41] water would perturb the molecular structure of the outermost surface comprising *p*-oxy azobenzene units of CRA-CMs more efficiently than NPC-02 would.

To evaluate the surface events after oblique irradiation with UV light, the contact angle hysteresis of CRA-CM monolayers of *Z*-isomers was examined. In the case of water as a probe liquid (open circles in Fig. 9(a)), the hysteresis of the monolayer of **2** was greatly reduced (*ca.* 20°), mainly owing to the increase in θ_r. In contrast, an apparent change in hysteresis was not observed for the monolayer of **1** even after exposure to UV light. A similar tendency was also observed using a probe liquid of NPC-02 (open circles in Fig. 9(b)). Interestingly, the results obtained from NPC-02 are well consistent with the photo-

Fig. 8 Wetting properties of mixed monolayers of **1** and **2**: advancing (θ_a; circles) and receding (θ_r; triangles) contact angles for (a) water and (b) NPC-02 before (filled) and after (open) exposure to UV light of a 0.2 J cm^{-2} exposure dose. The contact angle values were within an experimental error of $\pm 2°$.

Fig. 9 Wetting properties of mixed monolayers of **1** and **2**: contact angle hysteresis ($\theta_a - \theta_r$) of mixed monolayers of **1** and **2** for (a) water and (b) NPC-02 before (filled) and after (open) exposure to UV light of a 0.2 J cm^{-2} exposure dose. The solid (*E*-isomer) and dotted lines (*Z*-isomer) are included simply as guides to the eye.

Table 1 Summary of physicochemical properties of CRA-CM monolayers and LC alignments on the monolayers before and after photoirradiation

Photochemical state	Monolayer	Z-isomer (%)	Contact angle hysteresis for NPC-02	LC alignment state	LC/monolayer interface[a]
E	**1**				
	1 + 2	0	High	Homeotropic	
	2				(0)
Z	**1**	65	High	Homeotropic	
	1 + 2	65 < x < 92	High	Tilted	(0)
	2	92	Low	Homogeneous	(0)

[a]Open shapes indicate liquid crystal; filled shapes represent azobenzene; the substrate is represented by the flat surface below

induced LC alignment behaviors on the monolayers; the monolayers of $\chi(2)_{monolayer} = 0$, 0.50, 0.67 and 0.80 exhibited either homeotropic alignment or high pretilt angle even upon irradiation with UV light, while the monolayer of $\chi(2)_{monolayer} = 1$ caused the LC alignment alteration from homeotropic to homogeneous alignment (Fig. 7).

Because we compare the contact angle hystereses before and after photoisomerization of the same surface, it is obvious that the changes in hysteresis observed are not attributable to changes in macroscopic roughness or heterogeneity of CRA-CM monolayers. We believe that the changes in hysteresis are caused by alterations in molecular-level morphology and rigidity of CRA-CM monolayers. E-to-Z photoisomerization of azobenzenes tethered to a solid surface induces changes not only in the molecular-level morphology of the outermost surface but also in the degree of aggregation of the alkylazobenzene units because of changes in their orientational direction and geometry. Detailed insight into the relationship between the contact angle hysteresis and morphology of solid surfaces has been discussed.[18,42–44] For example, Fadeev and McCarthy found that the contact angle hysteresis of various kinds of alkylsilane monolayers is in reasonable agreement with their molecular-level topography and rigidity.[44] They insist that the hysteresis is small when the monolayers are flexible or packed densely to form smooth surfaces, but larger when the monolayers are rigid and have less ability to form smooth surfaces.

On the basis of the results of the contact angle hysteresis for CRA-CM monolayers, the origin of the LC alignment alterations observed can be rationalized by the photoinduced morphology changes of the monolayer surfaces. Homeotropic alignments or high pretilt angles observed in the monolayers of $\chi(2)_{monolayer} = 0$, 0.50, 0.67 and 0.80 in Z-state (Fig. 7) arise from intimate molecular interactions between the LC molecules and the molecular-level rough (rigid) azobenzene monolayers,[44] which thereby cause relatively large hysteresis (open circles in Fig. 9(b)). The insensibility of LC photoalignment and no marked alteration in contact angle hysteresis of monolayers containing **1** upon irradiation with UV light are interpreted as follows. Because the perfluorooctyl chains of **1** have characteristics such as a low surface free energy and molecular rigidity, it is reasonable to assume that the perfluoroalkyls are still exposed to an external phase regardless of the formation of polar Z-azobenzene after the photoisomerization. Therefore, no significant alteration to affect molecular-level morphological

heterogeneity to give rise to out-of-plane LC alignment occurs in the outermost surfaces of these monolayers. On the other hand, in the case of the monolayer of $\chi(2)_{monolayer} = 1$, the contact angle hysteresis was markedly decreased after photoisomerization, probably due to the high level of photoisomerization of the azobenzene units of **2** and the increase in the liquid-like character of the outermost surface comprising azobenzene units.[45] This indicates that the surface showing a low pretilt angle is topographically flat and less rigid.

In summary, the molecular-level roughness and fluidity deduced from the contact angle hysteresis is the most important factor to determine the photoinduced LC alignment transitions assisted by the CRA-CM monolayers. For the three-dimensional photoalignment of LCs by the CRA-CM monolayers, we insist that the inclined homeotropic alignment of LCs is generated preferentially by molecular-level rough surfaces and that the homogeneous alignment stems from a topographically flat (flexible) surface. This conclusion may be direct evidence that the molecular interdigitation of surface azobenzene residues with LC molecules, which leads to favored interfacial entropy, dominates homeotropic alignment of LCs.[46]

Conclusions

The three-dimensional orientation of LCs on substrates modified with CRA-CM monolayers can be manipulated by photoirradiation of the substrates with oblique non-polarized UV light. The photogenerated LC alignments are considerably influenced by the surface compositions of the monolayers. When LC cells modified with monolayers of CRA-CM with p-octylazobenzenes (**2**) are subjected to oblique irradiation with non-polarized UV light, the orientation of LC molecules is converted into homogeneous alignments tilting toward the direction of light propagation. On the other hand, single-component and mixed monolayers of CRA-CM with p-perfluorooctylazobenzene units (**1**) cause homeotropic alignments and high pretilt angles, respectively. Such contrasting behavior is not explained in terms of the level of photoisomerization and dipole–dipole interactions between LCs and surface alkylazobenzene residues. A clue to elucidate the photoalignment mechanism is obtained by the fact that the wetting properties of a liquid on a surface are very sensitive to details of the surface structure. We conclude that the molecular-level morphology and/or fluidity of the monolayer surfaces of CRA-CMs, which is deduced from the contact angle

hysteresis of the surfaces, is the most significant factor to cause the LC alignment alterations observed. This idea would be applied to understand the different behavior in the ability to perform three-dimensional LC photoalignment between SAMs and polymer thin films bearing azobenzene moieties. The principal results presented here are summarized in Table 1.

Acknowledgements

References

1   B. Jérôme, in *Handbook of Liquid Crystals*, ed. D. Demus, J. Goodby, G. W. Gray, H.-W. Spiess and V. Vill, Wiley-VCH, Weinheim, 1999, vol. 2, pp. 535–548; B. Jérôme, *Rep. Prog. Phys.*, 1991, **54**, 391.

2   J. Cognard, *Mol. Cryst. Liq. Cryst., Suppl. Ser.*, 1982, **1**, 1.

3   R. R. Shah and N. L. Abbott, *J. Am. Chem. Soc.*, 1999, **121**, 11300.

4   V. K. Gupta and N. L. Abbott, *Langmuir*, 1999, **15**, 7213.

5   V. K. Gupta, J. J. Skaife, T. B. Dubrovsky and N. L. Abbott, *Science*, 1998, **279**, 2077.

6   D. W. Berreman, *Phys. Rev. Lett.*, 1972, **28**, 1683.

7   J. M. Geary, J. W. Goody, A. R. Kmetz and J. S. Patel, *J. Appl. Phys.*, 1987, **62**, 4100.

8   W. Chen, M. B. Feller and Y. R. Shen, *Phys. Rev. Lett.*, 1989, **63**, 2665.

9   K. Ichimura, *Chem. Rev.*, 2000, **100**, 1847; K. Ichimura, in *Organic Photochromic and Thermochromic Compounds*, ed. J. C. Crano and R. J. Guglielmetti, Kluwer Academic/Plenum Publishers, New York, 1999, vol. 2, pp. 9–63.

10 M. O'Neill and S. M. Kelly, *J. Phys. D: Appl. Phys.*, 2000, **33**, R67.

11 K. Ichimura, Y. Suzuki, T. Seki, A. Hosoki and K. Aoki, *Langmuir*, 1988, **4**, 1214; K. Aoki, T. Seki, Y. Suzuki, T. Tamaki, A. Hosoki and K. Ichimura, *Langmuir*, 1992, **8**, 1007; Y. Kawanishi, T. Tamaki, M. Sakuragi, T. Seki, Y. Suzuki and K. Ichimura, *Langmuir*, 1992, **8**, 2601.

12 K. Ichimura, Y. Suzuki, T. Seki, Y. Kawanishi and K. Aoki, *Makromol. Chem., Rapid Commun.*, 1989, **10**, 5.

13 T. Seki, M. Sakuragi, Y. Kawanishi, Y. Suzuki, T. Tamaki, R. Fukuda and K. Ichimura, *Langmuir*, 1993, **9**, 211.

14 K. Ichimura, S. Morino and H. Akiyama, *Appl. Phys. Lett.*, 1998, **73**, 921.

15 S. Furumi, M. Nakagawa, S. Morino, K. Ichimura and H. Ogasawara, *Appl. Phys. Lett.*, 1999, **74**, 2438.

16 A. W. Adamson and A. P. Gast, *Physical Chemistry of Surfaces*, John Wiley & Sons, New York, 1997; *Contact Angle, Wettability and Adhesion*, ed. K. L. Mittal, VSP, Utrecht, 1993.

17 (*a*) C. D. Bain and G. M. Whitesides, *Angew. Chem., Int. Ed. Engl.*, 1989, **28**, 506; (*b*) G. M. Whitesides and P. E. Laibinis, *Langmuir*, 1990, **6**, 87.

18 (*a*) S. R. Holmes-Farley, R. H. Reamey, T. J. McCarthy, J. Deutch and G. M. Whitesides, *Langmuir*, 1985, **1**, 725; (*b*) C. D. Bain and G. M. Whitesides, *J. Am. Chem. Soc.*, 1988, **110**, 3665; (*c*) C. D. Bain and G. M. Whitesides, *J. Am. Chem. Soc.*, 1988, **110**, 5897; (*d*) C. D. Bain, J. Evall and G. M. Whitesides, *J. Am. Chem. Soc.*, 1989, **111**, 7155; (*e*) C. D. Bain and G. M. Whitesides, *J. Am. Chem. Soc.*, 1989, **111**, 7164; (*f*) P. E. Laibinis, R. G. Nuzzo and G. M. Whitesides, *J. Am. Chem. Soc.*, 1992, **114**, 1990; (*g*) P. E. Laibinis and G. M. Whitesides, *J. Phys. Chem.*, 1992, **96**, 5097.

19 M. Graupe, M. Takenaga, T. Koini, R. Colorado and T. R. Lee, *J. Am. Chem. Soc.*, 1999, **121**, 3222.

20 L. T. Creagh and A. R. Kmetz, *Mol. Cryst. Liq. Cryst.*, 1973, **24**, 59.

21 (*a*) R. A. Drawhorn and N. L. Abbott, *J. Phys. Chem.*, 1995, **99**, 16511; (*b*) V. K. Gupta and N. L. Abbott, *Langmuir*, 1996, **12**, 2587; (*c*) W. J. Miller, V. K. Gupta, N. L. Abbott, M.-W. Tsao and J. F. Rabolt, *Liq. Cryst.*, 1997, **23**, 175.

22 K. Ichimura, S.-K. Oh, M. Fujimaki, Y. Matsuzawa and M. Nakagawa, *J. Inclusion Phenomena Macrocycl. Chem.*, 1999, **35**, 173.

23 A. Kumar and G. M. Whitesides, *Appl. Phys. Lett.*, 1993, **63**, 2002; A. Kumar, H. A. Biebuyck and G. M. Whitesides, *Langmuir*, 1994, **10**, 1498; Y. Xia, M. Mrksich, E. Kim and G. M. Whitesides, *J. Am. Chem. Soc.*, 1995, **117**, 9576; L. B. Goetting, T. Deng and G. M. Whitesides, *Langmuir*, 1999, **15**, 1182.

24 Y. Xia and G. M. Whitesides, *Angew. Chem,. Int. Ed.*, 1998, **37**, 550.

25 T. J. Scheffer and J. Nehring, *J. Appl. Phys.*, 1977, **48**, 1783.

26 T. Tadokoro, T. Fukuzawa and H. Toriumi, *Jpn. J. Appl. Phys.*, 1997, **36**, L1207.

27 S.-K. Oh, M. Nakagawa and K. Ichimura, *Chem. Lett.*, 1999 349.

28 M. Fujimaki, S. Kawahara, Y. Matsuzawa, E. Kurita, Y. Hayashi and K. Ichimura, *Langmuir*, 1998, **14**, 4495; K. Ichimura, N. Fukushima, M. Fujimaki, S. Kawahara, Y. Matsuzawa, Y. Hayashi and K. Kudo, *Langmuir*, 1997, **13**, 6780.

29 C. H. Arrington, Jr. and G. D. Patterson, *J. Phys. Chem.*, 1953, **57**, 247; N. Higashi and T. Kunitake, *Chem. Lett.*, 1986, 105.

30 D. M. Small, *Handbook of Lipid Research 4. The Physical Chemistry of Lipids From Alkanes to Phospholipids*, Plenum Press, New York, 1986.

31 M. A. Bouchiat and D. Langevin-Cruchon, *Phys. Lett.*, 1971, **34A**, 331.

32 M. G. J. Gannon and T. E. Faber, *Philos. Mag.*, 1978, **37**, 117.

33 G. Möller, M. Harke, H. Motschmann and D. Prescher, *Langmuir*, 1998, **14**, 4955.

34 L. M. Siewierski, W. J. Brittain, S. Petrash and M. D. Foster, *Langmuir*, 1996, **12**, 5838.

35 A. B. D. Cassie, *Discuss. Faraday Soc.*, 1948, **3**, 11.

36 J. N. Israelachvili and M. L. Gee, *Langmuir*, 1989, **5**, 288.

37 K. Aoki, Y. Kawanishi, T. Seki, M. Sakuragi, T. Tamaki and K. Ichimura, *Liq. Cryst.*, 1995, **19**, 119.

38 Y. L. Chen, C. A. Helm and J. N. Israelachvili, *J. Phys. Chem.*, 1991, **95**, 10736.

39 H. Yoshizawa, Y.-L. Chen and J. Israelachvili, *J. Phys. Chem.*, 1993, **97**, 4128.

40 A. M. Schwartz, *J. Colloid Interface Sci.*, 1980, **75**, 404.

41 W. R. Brode, I. L. Seldin, P. E. Spoerri and G. M. Wyman, *J. Am. Chem. Soc.*, 1955, **77**, 2762.

42 P. A. DiMilla, J. P. Folkers, H. A. Biebuyck, R. Härter, G. P. López and G. M. Whitesides, *J. Am. Chem. Soc.*, 1994, **116**, 2225.

43 W. Jin, J. Koplik and J. R. Banavar, *Phys. Rev. Lett.*, 1997, **78**, 1520.

44 A. Y. Fadeev and T. J. McCarthy, *Langmuir*, 1999, **15**, 3759.

45 T. Seki, H. Sekizawa and K. Ichimura, *Polymer*, 1997, **38**, 725.

46 M. Büchel, B. Weichart, C. Minx, H. Menzel and D. Johannsmann, *Phys. Rev. E*, 1997, **55**, 455.